Quantitative Assessment for Commutation Security Based on Extinction Angle Trajectory

Qi Tao and Yusheng Xue

Abstract—**In order to reduce the risk of commutation failure (CF) in the AC/DC hybrid power system, the quantitative analysis on CF is required for on-line assessment and optimal control. This paper presents an accurate and reliable method to quantify the commutation security based on the trajectory due to the complexity of the high-voltage direct current (HVDC) model. Firstly, the characteristics of the extinction angle trajectory are analyzed under both commutation success and failure conditions. The commutation security margin index (CSMI) is then proposed for the HVDC systems. Moreover, a search strategy for parameter limits is put forward based on the sensitivity analysis of CSMI to accelerate the search speed with a guaranteed accuracy level. A modified IEEE 39-bus power system and an actual large-scale power system with 46 generators and 821 buses are utilized to verify the validity and robustness of the proposed index and strategy.**

Index Terms—**AC/DC hybrid power system, commutation failure (CF), commutation security margin, high-voltage direct current (HVDC), security limit.**

I. Introduction

HIGH-VOLTAGE direct current (HVDC) transmission system based on line-commutated converter (LCC) technology has been widely utilized to deliver clean energy from the western China to the eastern China [1], [2]. However, voltage reduction at the inverter side may lead to the simultaneous and successive commutation failure (CF) and even the forced blocking of converter stations. From 2011 to 2018, a total number of 60 CFs were recorded in the eastern China power grid, and up to four HVDC systems failed to commutate in the severest case. For the receiving side of AC power system, large amounts of thermal power plants have been retired in the face of bulk power imported via DC links, which leads to a continuous decline of the frequency regulation capacity. Therefore, the temporary power shortage would lead to a significant reduction of frequency and even trigger low-frequency load shedding. For the sending side of AC power system with weak network structure, the large-scale transfer of power flow to the adjacent AC transmission lines may deteriorate the power angle stability [3].

The suppression of CF is important to reduce the risk of DC blocking and increase the transmission capacity of HVDC links. So far, there have been a number of solutions to reduce the risk of CF, which can be classified as follows: the modification of converter topology [3]-[5], the improvement of voltage stability [6], [7], the modification of HVDC control systems [8]-[12], and the application of system emergency control strategies [13], [14], etc. However, the determination of control quantity and control time as well as the assessment of control effects depends on the accurate judgment and evaluation of CF.

There have been a lot of researches on the evaluation of CF. Under the assumption of an infinite AC bus, [15] presented a quasi-steady state model to calculate the critical converter bus voltage reduction as CF criterion. On this basis, [16], [17] improved the criterion by considering the post-fault DC current variation, occurrence moment of AC fault, and the speed of converter bus voltage drop. Inspired by the multi-infeed interaction factor (MIIF), [18] proposed the critical AC/DC voltage interaction factor (CADVIF) based on the equivalent impedance matrix of the receiving AC system, which was used as CF criterion for multi-infeed HVDC systems. However, since the dynamic characteristics of AC/DC systems in different fault scenarios are ignored, there should be certain discrepancies between these indices and the actual values. To address these concerns, the CF immunity index (CFII) was proposed in [19] based on the critical fault grounding impedance at the converter bus. However, this index needs to be conducted by simulation tools, thereby inevitably leading to heavy workload and long computation time. Reference [20] tried to accelerate the calculation speed of CFII by using the directrix relationship between CFII and effective short-circuit ratio (ESCR). Reference [21] deduced the analytical expression of CFII in a multi-infeed HVDC system based on the Thevenin equivalent circuit. Nevertheless, the above two methods were verified in a synthetic dual-infeed HVDC system, rather than actual ones. Based on a simplified two-machine system, [22] proposed an assessment criterion for CF which considered the voltage drop, the phase shift, and the spatial-temporal discreteness of AC system faults. But the misjudgment still exists, when this method is applied to the large system.

Existing studies on CF assessment focus on evaluating the

Manuscript received: December 31, 2019; accepted: June 4, 2020. Date of CrossCheck: June 4, 2020. Date of online publication: August 10, 2020.

Q. Tao and Y. Xue (corresponding author) are with the School of Electrical Engineering, Zhejiang University, Hangzhou 31000, China, and they are also with NARI Group Corporation (State Grid Electric Power Research Institute), Nanjing 21000, China (e-mail: taoqi_1991@126.com; xueyusheng@sgepri.sgcc.com.cn).

DOI: 10.35833/MPCE.2019.000239

ability of HVDC system to resist CF. Meanwhile, these indicators all depend on the parameter limit, which are mainly obtained by two ways: the first is to deduce the parameter limit analytically based on simplified system models; the second is to search the parameter limit by numerical simulation in a brute force way. The former ignores the dynamic characteristics of AC/DC hybrid power systems, while the latter is associated with massive computation costs. Therefore, it is necessary to propose an accurate method to evaluate the commutation process and a search strategy for parameter limit, which can reduce the computation costs on the premise of ensuring the accuracy.

Similar to static security analysis, the parameter limit of transient security analysis can be obtained either by trial and error or by sensitivity analysis technology, which needs a reliable quantitative index. Since the disturbed trajectories obtained by numerical simulation could include any factor, [23] proposed an evaluation scheme to extract quantitative information from trajectories directly. Several quantitative evaluation indices including power angle stability [23], voltage stability [24], frequency stability [25] have been developed and applied into practical projects [26], [27]. Inspired by these work, the commutation security margin index (CSMI) is proposed in this paper. Considering that the extinction angle criterion is the essence of CF [28], CSMI is obtained based on the characteristics of extinction angle trajectory in the cases of commutation success and failure. This index can not only reflect whether the converter fails to commutate, but also make accurate estimate of the security degree of the commutation. As the index is extracted from the trajectory, it is convenient to incorporate complex factors such as device models and fault scenarios. Moreover, the index can be applied to any commutation process such as the simultaneous/successive CF of different HVDC systems. The monotone and smooth variations of index-parameter curve are advantageous to speed up the search process based on sensitivity analysis, which is especially helpful for online analysis and control operation of AC/DC hybrid transmission system.

This paper is organized as follows. Section II presents the quantitative analysis method for commutation security based on the trajectory. Section III elaborates on the calculation methods for CSMI in the cases of commutation success and failure. In Section IV, a sensitivity-based strategy is proposed to search for the parameter limit in the AC/DC hybrid power system. In Section V, the effectiveness of the index and the rapidity of the search strategy are validated in a modified IEEE-39 bus system and an actual regional power system. Finally, Section VI concludes the paper.

II. Quantitative Analysis of Commutation Security

A. Complexity of DC Dynamic Model

Generally, strong random factors such as voltage phase shift and transient characteristics of trigger circuit can be ignored in the online assessment and control system. Therefore, the quasi-steady state model with the DC average output and the AC power-frequency positive-sequence quantities is adopted.

Since CF mainly occurs at the inverter side, the equations of the inverter model are represented as:

$$\begin{cases} U_{\mathrm{do}} = \dfrac{3\sqrt{2}\,U_{\mathrm{c}}}{k\pi} \\ U_{\mathrm{d}} = U_{\mathrm{do}}\cos\beta + d_{\mathrm{x}} I_{\mathrm{d}} \\ \gamma = \arccos\left(\dfrac{\sqrt{2}\,kI_{\mathrm{d}}X_{\mathrm{T}}}{U_{\mathrm{c}}} + \cos\beta\right) \\ \mu = \beta - \gamma \\ P_{\mathrm{d}} = U_{\mathrm{d}} I_{\mathrm{d}} \end{cases} \tag{1}$$

where U_{do} is the maximum average DC voltage; U_{c} is the root mean square value of line-to-line commutating voltage referred to the primary side of the converter transformer; k is the ratio of the converter transformer; U_{d} is the DC voltage; d_{x} is the equivalent commutation resistance; I_{d} is the DC current; X_{T} is the commutation reactance; β is the firing-advance angle; γ is the extinction angle; μ is the overlap angle; and P_{d} is the DC power.

The controllable device used in the converter of LCC-HVDC is thyristor valve. Because of the stored charges produced during the forward conduction interval, the valve cannot establish the forward voltage blocking capability immediately after the forward anode current cease to flow. If a forward voltage is reapplied prematurely to the valve, the device will go into the conduction state again [28]. The time required to remove the excess charges is defined as critical turn-off time, which is converted into electrical angle and termed as the critical extinction angle γ_{c} [29]. CF occurs when the actual extinction angle γ is less than γ_{c} [30]. In practice, the critical turn-off time is about 400 μs, which corresponds to about 7° in electrical angle for a 50 Hz AC power system. In this paper, the critical extinction angle of the simulation model $\gamma_{\mathrm{c,set}}$ is selected to be 7°。

The control system applied in the actual HVDC transmission projects mainly refers to the technological route in [31]. In Fig. 1, P_{ref} is the instruction of DC power from the dispatching center; I_0 is the instruction of DC current from the master controller; and α is the firing angle order for the rectifier. The DC control system consists of 8 submodules: master controller, voltage dependent current order limiter (VDCOL), current control amplifier (CCA), voltage controller, γ controller, rectifier α_{min} limiter, CF prevention control (CFPREV), and γ_0 controller.

CCA provides the corresponding fire angle orders to the converter, which are dynamically limited by the output of the other controller. The fire angle order of the inverter is limited by the outputs from γ controller and the voltage controller. The fire angle order is the minimum of the outputs from γ controller, the voltage controller, and CCA. If the thyristor valves commutate successfully, the output of γ controller is the minimum, namely the inverter is controlled by γ controller.

Under the assumption of quasi-steady state, the analytical analysis is still difficult to apply to the AC/DC hybrid power system. In addition to the differential-algebraic equations (DAEs), the difference equation and the logic language are needed to describe the control system. Therefore, the mathematical model of AC/DC hybrid power system is a set of logical-difference-differential-algebraic equations (LDDAEs). In order to analyze the commutation process accurately, the numerical simulation is inevitable.

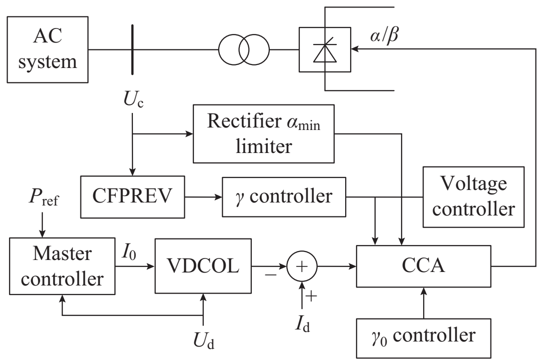

Fig. 1. Control logic of an HVDC system.

B. Analysis of Commutation Security Based on Trajectory

At present, the extinction angle trajectory obtained by the time-domain simulation is mainly used to judge whether the inverter succeeds to commutate. Based on this qualitative analysis method, the parameter limit can only be obtained by trial and error, which is difficult to be applied to online analysis and optimal control. In order to use the sensitivity analysis method to search the parameter limit, a quantitative index is required to evaluate the commutation security under specified operation conditions and fault scenarios. Therefore, a quantitative evaluation method of commutation security is put forward based on the extinction angle trajectory.

The extinction angle trajectories will vary with the system or fault parameters. α_{cr} is the parameter limit for the critical case. Figure 2 depicts the typical extinction angle trajectories of commutation success. If CF does not occur, the extinction angle in the simulation is always larger than the set critical extinction angle $\gamma_{c,set}$. When CF is about to happen, the minimum value of the extinction angle trajectory γ_{min} should be equal to $\gamma_{c,set}$. Therefore, the difference $\Delta\gamma_{min}$ between γ_{min} and $\gamma_{c,set}$ in Fig. 2 reflects the distance between the current commutation and the critical state.

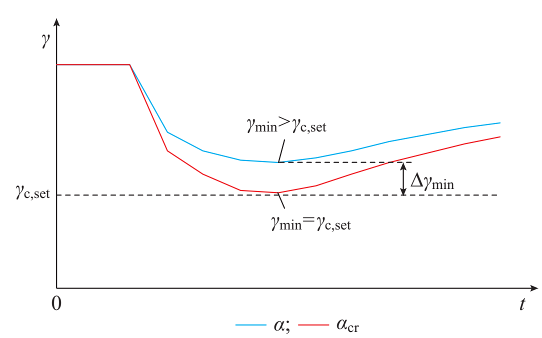

Fig. 2. Quantitative assessment for commutation security based on extinction angle trajectory under commutation success.

The typical extinction angle trajectory of CF is depicted in Fig. 3. Once CF occurs, γ_{min} of the extinction angle trajectory would always drop to 0, which means that $\Delta\gamma_{min}$ cannot reflect the severity of CF in different situations. If there is a need to restore the CF into success, an additional commutation security margin can be provided by lower $\gamma_{c,set}$. Try to reduce $\gamma_{c,set}$ gradually in simulation until CF does not happen, $\gamma_{c,set}$ can be defined as the potential minimum extinction angle $\gamma_{min,pot}$, and the corresponding extinction angle trajectory can be defined as the potential extinction angle trajectory, as shown in Fig. 3. Similar to the case of commutation success, $\Delta\gamma_{min,pot}$ can assess the severity of CF.

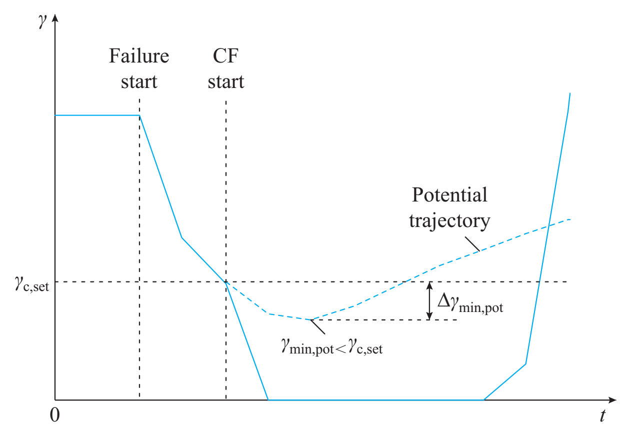

Fig. 3. Quantitative assessment for commutation security based on extinction angle trajectory under CF.

However, the method of obtaining $\Delta\gamma_{min,pot}$ by reducing $\gamma_{c,set}$ increases the computation cost and deviates from the original commutation process, which is difficult to be applied to multi-infeed DC systems and the successive CF. Therefore, it is necessary to estimate $\Delta\gamma_{min,pot}$ by another characteristic quantity that can be observed and is positively correlated with $\Delta\gamma_{min,pot}$.

Since the topology and control strategy of the DC model are different before and after CF, it is necessary to select the extinction angle trajectory before CF to extract characteristic quantity. The extinction angle trajectory before the fault is mainly determined by the γ controller and is not affected by the fault parameters. Thus the middle trajectory is suitable to evaluate the severity of CF.

Figure 4 depicts the variation of potential extinction angle trajectories with the parameter, in which the overlap between the potential trajectory and the actual trajectory is marked by solid lines. When the parameter α takes different values α_i and α_j, it is assumed that the potential minimum extinction angle $\Delta\gamma_{min,pot}$ satisfies the following relationship:

$$\begin{cases} \Delta\gamma_{min,pot}(\alpha_i)<\Delta\gamma_{min,pot}(\alpha_j) \\ \Delta\gamma_{min,pot}(\alpha_{cr})=0 \end{cases} \tag{2}$$

where $\Delta\gamma_{min,pot}(\cdot)$ is the value of $\Delta\gamma_{min,pot}$ for different parameter α.

In general, the extinction angle trajectory meets the following characteristics.

Characteristic 1: the time interval $\Delta t(\alpha)$, which is between the start time of CF and the time for the trajectory to reach the minimum value $\gamma_{\text{min, pot}}$, increases as $\Delta\gamma_{\text{min, pot}}$ decreases:

$$\begin{cases}\Delta t(\alpha_i) > \Delta t(\alpha_j) \\ \Delta t(\alpha_{\text{cr}}) = 0\end{cases} \tag{3}$$

where $\Delta t(\cdot)$ is the value of Δt for different parameter α.

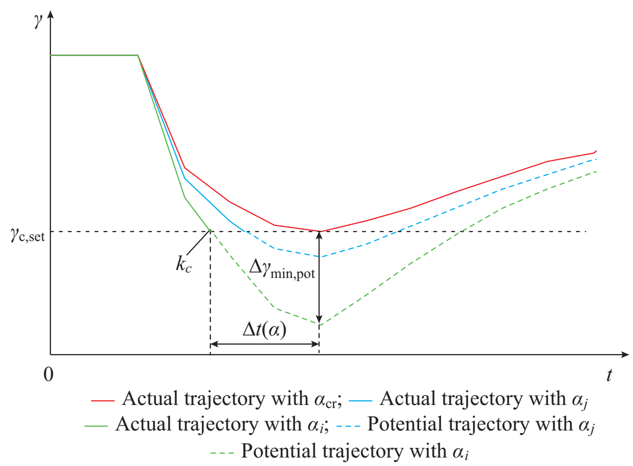

Fig. 4. Characteristic quantities of potential extinction angle trajectories with different parameters.

Characteristic 2: the changing rate of the potential extinction angle trajectory varies continuously with time, and becomes 0 at the minimum value. Since there are a large number of inductors and capacitors in AC/DC hybrid system to suppress the saltation of voltage and current [17] and the proportional integral (PI) control adopted by the DC controller can keep the fire angle order changing gently in steady state [32], the change rate of the extinction angle trajectory is continuous when CF does not occur. Consequently, before reaching the minimum value, the change rate of the potential extinction angle trajectory will gradually decrease. The first-order sensitivity coefficient $k(t)$ of the trajectory will gradually increase with time:

$$k(t) < k(t + \Delta t) \tag{4}$$

Substituting (3) into (4), the larger Δt is, the smaller the first-order sensitivity coefficient k_c of the trajectory at $\gamma_{\text{c, set}}$ is. The variation of k_c with α satisfies:

$$\begin{cases}k_c(\alpha_i) < k_c(\alpha_j) \\ k_c(\alpha_{\text{cr}}) = 0\end{cases} \tag{5}$$

where $k_c(\cdot)$ is the value of k_c for different parameter α.

According to (2) and (5), the changing trend of $\Delta\gamma_{\text{min, pot}}$ and k_c with the α is consistent. Hence k_c is positively correlated with $\Delta\gamma_{\text{min, pot}}$. Meanwhile, in the critical situation, k_c is equal to 0. When CF occurs, k_c is less than 0. Therefore, k_c can be used to estimate $\Delta\gamma_{\text{min, pot}}$ and reflect the severity of CF.

III. Calculation Method of CSMI Based on Trajectory

A. Requirements for CSMI

This paper proposes CSMI based on the extinction angle trajectory, which is the foundation of obtaining the parameter limit and the parameter margin with sensitivity analysis technology. According to the requirements of trajectory margin in [23], CSMI should also meet the following requirements: ① there is one and only one margin index for certain operation conditions and fault scenarios; ② the margin index can strictly reflect the necessary and sufficient conditions for CF; ③ the securer the commutation process is, the higher the margin index is, and vice versa; ④ the margin index can reflect any change of parameters; ⑤ the margin index varies continuously and smoothly with the parameter.

B. Calculation Method of CSMI for Commutation Success

According to the characteristics of the extinction angle trajectory, CSMI in the case of success can be directly obtained based on γ_{min} of the extinction angle trajectory in the observation time window. The calculation equation is expressed as:

$$\Delta\gamma_{\text{min}} = \gamma_{\text{min}} - \gamma_{\text{c, set}} \tag{6}$$

Most CFs are caused by voltage disturbances originated from AC system faults, thus the existing research works use the fault impedance Z_{f} as the typical parameter to study CF [19]. An example is given in Fig. 5, when Z_{f} takes different values, $\Delta\gamma_{\text{min}}$ changes monotonically and smoothly with Z_{f}.

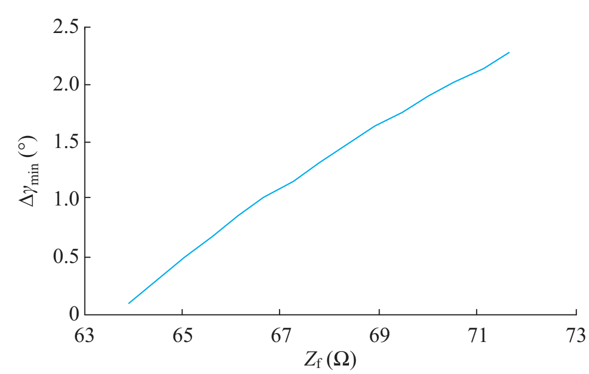

Fig. 5. Relationship between $\Delta\gamma_{\text{min}}$ and Z_{f} for commutation success.

C. Calculation Method of CSMI for CF

For the case of CF, there are two key steps to calculate the CSMI: calculate the first-order sensitivity coefficient k_c of the extinction angle trajectory, and use k_c to estimate $\Delta\gamma_{\text{min, pot}}$.

1) Calculation of k_c

In the ideal situation, the first-order sensitivity coefficient k_c of the extinction angle trajectory at $\gamma_{\text{c, set}}$ can be obtained as:

$$k_c = \frac{\gamma(t_1) - \gamma(t_2)}{t_1 - t_2} \tag{7}$$

where $\gamma(\cdot)$ is the value of γ for different time; t_2 is the time when CF occurs; $\gamma(t_2)$ is equal to $\gamma_{\text{c, set}}$; and $t_1 = t_2 - \Delta t$ and Δt approaches to 0.

However, the extinction angle trajectory obtained by simulation is composed of discrete value $\gamma(t)$, as shown in Fig. 6. In this case, $\gamma(t_1)$ and $\gamma(t_2)$ in (7) are the extinction angle of two integral steps before and after CF, and Δt is the integral step size. Since the step size of electromechanical transient simulation is large, $\gamma(t_2)$ cannot be exactly equal to $\gamma_{c,set}$, and Δt does not approach to 0. The above factors will introduce errors, and result in poor smoothness of the original k_c curve in Fig. 7, when Z_f is taken as the parameter variable. These errors can be eliminated by reducing the integral step size.

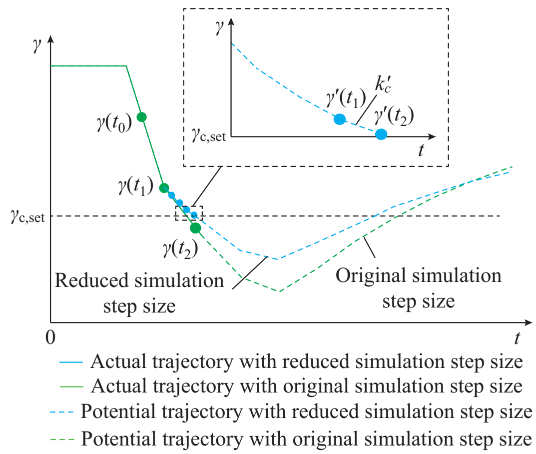

Fig. 6. Calculation method of k_c.

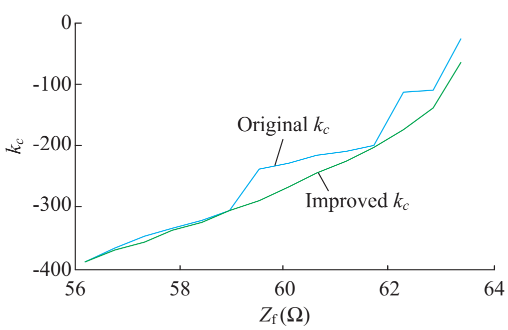

Fig. 7. Comparison between curves of original k_c and improved k_c varying with Z_f.

A feasible solution is proposed in Fig. 6. After CF is confirmed with the original step size, the simulation can restart with a smaller step size from the former step before CF until it happens again. By reducing the step size within only one original step, a more accurate k_c' can be obtained with little computation cost.

However, the commercial simulation software has a limited capability of variable step-size simulation. Since the reduction of simulation step size is not always feasible, another improved calculation method of k_c is proposed. Similar to (7), the first-order sensitivity coefficient at time t_1 and t_2 can be obtained as:

$$\begin{cases} k(t_1)=\dfrac{\gamma(t_0)-\gamma(t_1)}{t_0-t_1} \\ k(t_2)=\dfrac{\gamma(t_1)-\gamma(t_2)}{t_1-t_2} \end{cases} \tag{8}$$

According to the second characteristic of the extinction angle trajectory, $k(t)$ varies with the time continuously. Assuming that $k(t)$ in an integral step changes linearly with the time, the improved k_c can be defined as:

$$k_c=\frac{\gamma(t_2)-\gamma_{c,set}}{\gamma(t_2)-\gamma(t_1)}k(t_1)+\frac{\gamma_{c,set}-\gamma(t_1)}{\gamma(t_2)-\gamma(t_1)}k(t_2) \tag{9}$$

The smoothness of the improved k_c curve is greatly improved in Fig. 7.

2) Estimation of $\Delta\gamma_{min,pot}$

Given that variation trends of $\Delta\gamma_{min,pot}$ and $\Delta\gamma_{min}$ with the parameter are the same, and k_c varies monotonically with the parameter, k_c can be used to estimate $\Delta\gamma_{min,pot}$ based on linear or quadratic fitting. Taking the linear fitting method as an example, the method of estimating $\Delta\gamma_{min,pot}$ with k_c is introduced. The equation of linear fitting can be expressed as:

$$\Delta\gamma_{min,pot}=\lambda k_c+\Delta\gamma \tag{10}$$

For the critical state, (10) can be satisfied as:

$$\begin{cases} \Delta\gamma_{min,pot}(\alpha_{cr})=0 \\ k_c(\alpha_{cr})=0 \end{cases} \tag{11}$$

Assuming that the change of extinction angle caused by $\Delta\alpha$ is the same, the relationship between parameters α_i^+, α_j^+, α_n^-, α_m^- and their $\Delta\gamma_{min}$, $\Delta\gamma_{min,pot}$ in Fig. 8 can be expressed as:

$$\frac{\Delta\gamma_{min}(\alpha_i^+)-\Delta\gamma_{min}(\alpha_j^+)}{\alpha_i^+-\alpha_j^+}=\frac{\Delta\gamma_{min,pot}(\alpha_n^-)-\Delta\gamma_{min,pot}(\alpha_m^-)}{\alpha_n^--\alpha_m^-} \tag{12}$$

Substituting (11) and (12) into (10), we can obtain:

$$\begin{cases} \lambda=\dfrac{(\Delta\gamma_{min}(\alpha_i^+)-\Delta\gamma_{min}(\alpha_j^+))/(\alpha_i^+-\alpha_j^+)}{(k_c(\alpha_n^-)-k_c(\alpha_m^-))/(\alpha_n^--\alpha_m^-)} \\ \Delta\gamma=0 \end{cases} \tag{13}$$

where λ is the conversion coefficient.

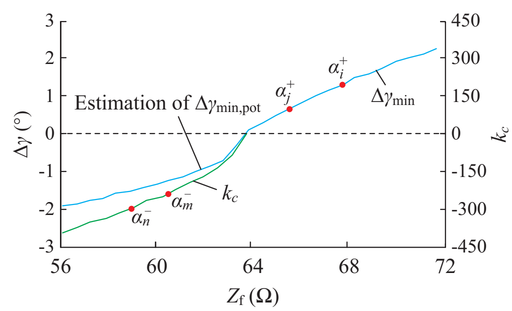

Fig. 8. Estimation of $\Delta\gamma_{min,pot}$ with k_c.

In order to improve the linearity and smoothness of the index-parameter curve near the critical parameter, the values of α_i^+, α_j^+, α_n^-, α_m^- should be as close as possible to the parameter limit α_{cr}. Figure 8 illustrates the variation of $\Delta\gamma_{min}$ and $\Delta\gamma_{min,pot}$ with Z_f, whose smoothness and linearity both meet the requirements of trajectory margin index.

D. Standardization of CSMI

In order to make CSMI comparable in different cases and different DC systems, the index is standardized in (14), where σ is defined as standardized CSMI. In the case of commutation success, σ at steady state is considered to be

100%. The extinction angle γ at steady state is fixed by the set value γ_{ref} of the γ controller, so $\gamma_{\mathrm{ref}}-\gamma_{\mathrm{c,set}}$ is taken as the reference value. In the case of CF, σ is considered to -100% when $\gamma_{\mathrm{min,pot}}$ is 0, so $\gamma_{\mathrm{c,set}}$ is taken as the base value. When the commutation state is critical, the results of both equations are 0. Without modifying the original definition, the standardization makes the margin index within the range of $(-100\%, 100\%)$.

$$\sigma=\begin{cases}\dfrac{\Delta\gamma_{\mathrm{min,pot}}}{\gamma_{\mathrm{c,set}}}\times 100\%=\dfrac{\lambda k_c}{\gamma_{\mathrm{c,set}}}\times 100\% & \text{CF}\\ \dfrac{\Delta\gamma_{\mathrm{min}}}{\gamma_{\mathrm{ref}}-\gamma_{\mathrm{c,set}}}\times 100\% & \text{commutation success}\end{cases} \tag{14}$$

IV. Parameter Limit Search Strategy Based on Sensitivity Analysis of CMSI

A. Interaction Between Multiple HVDC Systems

For a multi-infeed HVDC system, CF has a large active and reactive power impact on the AC system, which also affects the extinction angle characteristics of other HVDC systems. Since CF initially occurs in HVDC2, the monotonicity of the first-order sensitivity coefficient for the extinction angle trajectory of HVDC1 will be affected. It no longer meets the second characteristic of the extinction angle trajectory. Only the HVDC system with the earliest CF ensures that it will not be affected by other HVDC systems. Furthermore, k_c of its extinction angle trajectory changes monotonically with the parameter as shown in Fig. 9.

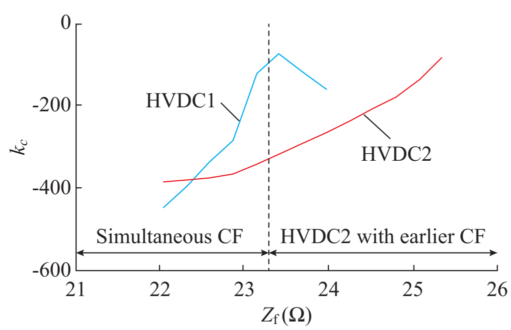

Fig. 9. Curves of k_c varying with Z_f for different HVDC systems.

Therefore, when searching for the parameter limit of a multi-infeed HVDC system, a suitable HVDC system should be selected as the search object. The selection principle is as follows:

1) If no CF occurs, the HVDC system with the smallest commutation security margin is selected as the search object.

2) If there is a CF, the only HVDC system that fails to commutate or the HVDC system with the earliest CF is selected as the search object.

B. Search Strategy

Based on the sensitivity analysis of CSMI, a parameter limit search strategy is proposed for the multi-infeed HVDC system. This strategy can also be applied to the single-infeed HVDC system, which is a special case of the multi-infeed HVDC system. The search strategy is proposed on the premise that σ is proportional to α. For the opposite case, it can also work in a similar way. The steps of the parameter limit search strategy are as follows:

Step 1: adaptive start. Set a conservative parameter range as $[\underline{\alpha},\bar{\alpha}]$. The simulation is carried out on the parameters $\underline{\alpha}$ and $\bar{\alpha}$, respectively. If both cases are commutation success or failure, it means that there is no parameter limit within this range. Therefore, the value range can be expanded appropriately, or the search is exited. Otherwise, the parameter limit can be searched within this range. When the parameter equals to $\underline{\alpha}$, σ can be considered to be -100%, so the initial conversion coefficient of each HVDC systems can be calculated as:

$$\lambda_i^1=-\gamma_{\mathrm{c.set}}/k_c(\underline{\alpha}) \tag{15}$$

Set iteration step as n=1.

Step 2: calculate CSMI. If there is no CF, the minimum value of the extinction angle trajectory γ_{min} is used to calculate the CSMI of commutation success. Otherwise, k_c of the extinction angle trajectory at $\gamma_{\mathrm{c,set}}$ and the conversion coefficient λ_i^n are used to calculate the CSMI of CF.

Step 3: select the HVDC system. According to the HVDC selection principle mentioned above, the HVDC system in the first iteration can be selected based on the simulation results of the parameter $\underline{\alpha}$ or $\bar{\alpha}$. In the subsequent search process, the HVDC system is selected according to the trajectory of the parameter limit $\alpha_{\mathrm{cr}}^{n-1}$, which is obtained in the previous iteration step.

Step 4: estimate the parameter limit. The parameter limit can be estimated based on the margin index of the selected HVDC system. In general, sensitivity analysis relies on numerical perturbations near the initial value, but it will increase unnecessary simulations. Therefore, the parameter limit α_{cr}^n can be linearly estimated by the previous margin indices. The essence of this method is the sensitivity estimation with the large step:

$$\alpha_{\mathrm{cr}}^n=\bar{\alpha}-\frac{\sigma_i(\bar{\alpha})}{\sigma_i(\bar{\alpha})-\sigma_i(\underline{\alpha})}(\bar{\alpha}-\underline{\alpha}) \tag{16}$$

where σ_i is CSMI of the selected HVDC systems; and $\sigma_i(\cdot)$ is the value of σ_i for different parameter α.

After the simulation based on α_{cr}^n, if the CF occurs, α_{cr}^n is used to update $\underline{\alpha}$. Otherwise, α_{cr}^n is used to update $\bar{\alpha}$.

Step 5: update conversion coefficient. Parameter limit α_{cr} is unknown during the search process. In order to ensure the linearity and smoothness of the index-parameter curve near the parameter limit, λ_i^n of each HVDC system needs to be updated during the search process. The parameters α_i^+, α_j^+, α_n^-, α_m^- in (12) should be updated with the previous estimated results which are close to the real α_{cr}.

Step 6: check the convergence. If the difference between the upper and lower limits of the updated value interval $|\bar{\alpha}-\underline{\alpha}|$ is less than the threshold ε_1, or the commutation success margin $\sigma_i(\bar{\alpha})$ is less than the threshold ε_2, terminate the search and take the latest estimated value α_{cr}^n as the result. Otherwise, set n=n+1 and go to *Step 2*.

V. Case Studies

In this section, the power system simulation is conducted in the PSD-BPA electromechanical transient simulation program, and the parameter limit search strategy in Fig. 12 is implemented in the MATLAB environment. The correctness and effectiveness of the proposed index and search strategy are verified by a modified IEEE 39-bus system with a single HVDC transmission line and an actual multi-infeed HVDC system.

A. Performance Evaluation of Sensitivity-based Search Strategy

Since the computation cost of the parameter limit search strategy is mainly contributed by the numerical simulation, we use the number of simulations to evaluate the computation cost. Among the parameter limit search methods based on qualitative criteria of the numerical simulation, the method with the least time cost is the dichotomy method [33], [34]. This method performs an interval-based search and determines an interval around the parameter limit with the qualitatively judgment whether the CF occurs. Successive iterations of the algorithm can cause the interval small enough to satisfy the desired accuracy. Therefore, the time cost of the proposed search strategy is compared with the dichotomy method. In order to illustrate the superiority of the method proposed in this paper in terms of convergence speed, the acceleration ratio ζ is defined as:

$$\zeta = \frac{\overline{N}_{BS}}{\overline{N}_{SS}} \tag{17}$$

where $\overline{N}_{SS}$ is the average simulation time of the sensitivity-based search strategy; and $\overline{N}_{BS}$ is the average simulation time of the dichotomy method.

B. Single-infeed HVDC System

The modification of the IEEE 39-bus system with single HVDC transmission line is shown in Fig. 10 and specified as follows: line between bus 23 and bus 24 is removed, the load of bus 24 is transferred to bus 23, and an HVDC transmission line is added on bus 24 to interconnect with the external power grid, which is represented by an infinite bus [35].

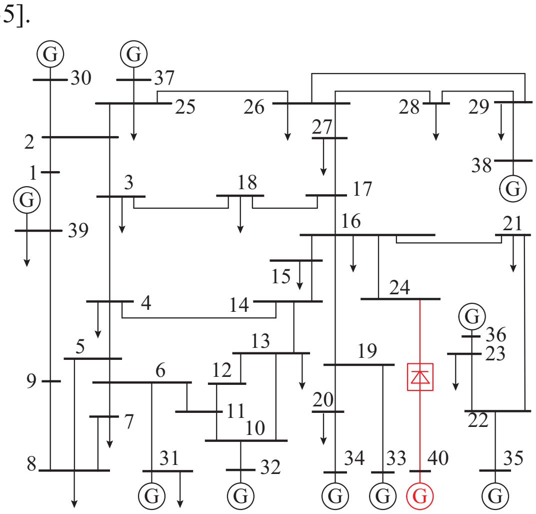

Fig. 10. Modified IEEE 39-bus system.

The rated power P_{dN} of the newly added HVDC system is 1000 MW. γ_{ref} during steady state operation is 17°. $\gamma_{c,set}$ is set as 7°. Reactive power compensation of converter station is provided by the filters, which follows the configuration principle that the reactive power between the converter station and the AC system is less than the capacity of a set of filters (50 Mvar). The HVDC power fed into the system is spread to buses 15, 16, 20, 21, 27 for dissipation. The generator conforms to a classic second-order model, and the load conforms to a constant impedance, constant current, constant power (ZIP) model (40% constant impedance +60% constant power).

In order to verify the applicability of the search strategy for different parameters, the typical search processes for the parameter limit such as grounding impedance Z_f, DC power P_d, and fault clearing time τ are given below. For all the cases, the convergence accuracy ε_1 is 1% of the relevant limit value, and ε_2 is 1%.

1) Fault Grounding Impedance

In this case, the fault type applied at bus 16 is a three-phase impedance grounding fault with a duration of 0.1 s, $[\underline{Z}_f, \overline{Z}_f] = [0, 0.1]$ p.u.. Table I shows the search process of Z_f limit and Fig. 11 presents the extinction angle trajectories and characteristic values during the iterative process. Since the corresponding margin index σ of $\underline{Z}_f$ is set as −100%, the initial conversion coefficient λ_1 can be calculated as 0.0021. According to the extinction angle trajectories of $\underline{Z}_f = 0$ p.u. and $\overline{Z}_f = 0.1$ p.u. in Fig. 11, it can be obtained that $\underline{\sigma} = -100\%$ and $\overline{\sigma} = 62.47\%$, respectively. Substituting them into (16), the first estimated value $Z^1_{f,cr}$ can be obtained as 0.0615 p.u.. The commutation process of $Z^1_{f,cr}$ is successful, and $\overline{Z}_f$ should be updated with $Z^1_{f,cr}$ for the next iteration. The subsequent search process is similar. After the second iteration, there are two extinction angle trajectories for each of the commutation success and failure, which can be used to update the new conversion coefficient $\lambda^3 = 0.0016$. When $Z^3_{f,cr} = 0.0523$ p.u., σ^3_{cr} is 0.71%, which is less than ε_2, the search process is over.

TABLE I
SEARCH PROCESS OF Z_f LIMIT

No.	λ	$\underline{Z}_f$ (p.u.)	$\underline{\sigma}$ (%)	$\overline{Z}_f$ (p.u.)	$\overline{\sigma}$ (%)	$Z^n_{f,cr}$ (p.u.)	σ^n_{cr} (%)
1	0.0021	0	−100.00	0.1000	62.47	0.0615	25.38
2	0.0021	0	−100.00	0.0615	25.38	0.0491	−8.66
3	0.0016	0.0491	−8.66	0.0615	25.38	0.0523	0.71

2) DC Power

P_d is an operation parameter, and its range depends on the operation condition. To avoid the intermittence of DC current caused by low DC power, set minimum power $\underline{P}_d$ as 10% of rated power P_{dN}. Considering the future expansion, set maximum power $\overline{P}_d$ as double rated power P_{dN}. In this case, P_{dN} is 1000 MW, hence $[\underline{P}_d, \overline{P}_d] = [100, 2000]$MW. The

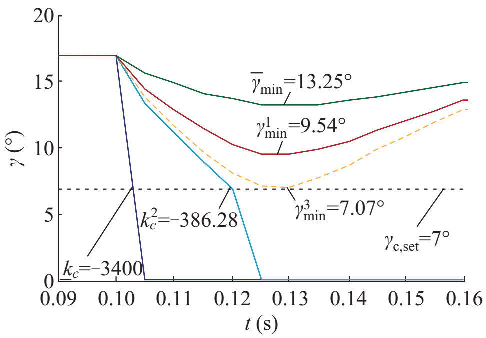

Fig. 11. Extinction angle trajectories in search for Z_f limit.

fault type applied at bus 8 is a three-phase impedance (0.04 p.u.) grounding fault with a duration of 0.1 s. Figure 12 and Table II show the search process of P_d limit, which is similar to the parameter Z_f. When $P^2_{d,cr} = 400$ MW, $\sigma^2_{cr} = 0.22\%$ is less than ε_2, the search process is over.

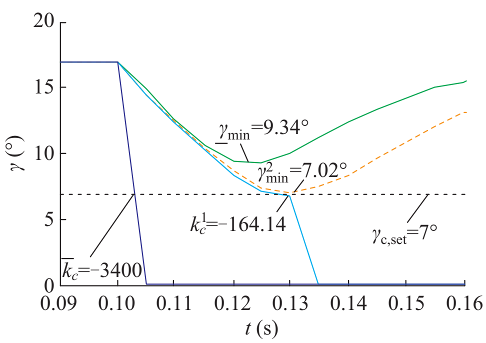

Fig. 12. Extinction angle trajectories in search for P_d limit.

TABLE II
SEARCH PROCESS OF P_d LIMIT

No.	λ	$\underline{P}_d$ (MW)	$\underline{\sigma}$ (%)	$\overline{P}_d$ (MW)	$\overline{\sigma}$ (%)	$P^n_{d,cr}$ (MW)	σ^n_{cr} (%)
1	0.0021	100	23.39	2000	−100.00	460	−4.83
2	0.0021	100	23.39	460	−4.83	400	0.22

3) Fault Clearing Time

τ is a fault parameter. Since the transient stability is the basic requirement for the operation, the upper limit can be set as the critical clearing time for the transient stability. When a zero-impedance three-phase grounding fault is applied at bus 13, the critical clearing time of the transient stability is 0.234 s. Set $[\underline{\tau}, \overline{\tau}] = [0, 0.234]$s. Unlike other parameters, τ only affects the commutation process after fault clearance. For the commutation process after fault clearance, the search process of τ limit is shown in Table III and Fig. 13. After the fourth iteration, the updated $[\underline{\tau}, \overline{\tau}] = [0.148, 0.149]$ s will cause $|\overline{\tau} - \underline{\tau}|/\tau^4_{cr}$ to be less than ε_1, then the search process is over.

In order to verify the impact of different fault locations on the robustness of the proposed strategy, 30 sets of examples are randomly selected for the above 3 typical parameters (10 sets respectively) in the modified IEEE 39-bus system. Parameter value range and convergence accuracy are consistent with typical examples. The statistical results of 30 examples are given in Table IV, where $\min(N_{SS})$ is the minimum number of simulations in all examples for different parameters, and $\max(N_{SS})$ is the maximum number. The computation cost of the proposed search strategy in this paper is less than the dichotomy method for all examples. The convergence speed has been increased by 50%-90% on average for different parameters, and the fastest case can be obtained in only one iteration (3 times of simulation).

TABLE III
SEARCH PROCESS OF CCT

No.	λ	$\underline{\tau}$ (s)	$\underline{\sigma}$ (%)	$\overline{\tau}$ (s)	$\overline{\sigma}$ (%)	τ^n_{cr} (s)	σ^n_{cr} (%)
1	0.0044	0	100.00	0.234	−100.00	0.117	52.58
2	0.0044	0.117	52.58	0.234	−100.00	0.157	−16.21
3	0.0027	0.117	52.58	0.157	−16.21	0.148	3.51
4	0.0104	0.148	3.51	0.157	−63.31	0.149	−3.11

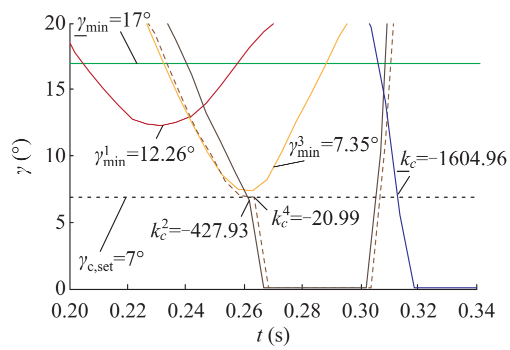

Fig. 13. Extinction angle trajectories in search for CCT.

TABLE IV
COMPARISON OF COMPUTATION COSTS IN MODIFIED IEEE 39-BUS SYSTEM

Parameter	$\overline{N}_{SS}$	$\overline{N}_{BS}$	$\min(N_{SS})$	$\max(N_{SS})$	ζ
Z_f	6.2	12.0	5	8	1.94
P_d	5.3	9.6	3	7	1.81
τ	6.9	10.5	5	9	1.52

C. Multi-infeed HVDC System

A regional power grid in eastern China is selected as the multi-infeed HVDC test system to verify the applicability of the proposed strategy in practical settings of the system size, model complexity, and multiple HVDC CFs. The grid contains 46 generators, 821 buses, and 4 HVDC transmission lines, six-order dual-axis generator model and dynamic load model are used in this system. Four HVDC transmission lines are ±500 kV Gezhouba-Nanqiao (GN), ±500 kV Yidu-Huaxin (YH), ±500 kV Tuanlin-Fengjing (TF) and ±800 kV Fulong-Fengxian (FF). Figure 14 shows the 500 kV AC network structure of this regional power grid.

In the search process of parameter limit for the multi-infeed HVDC system, if the selected HVDC system remains the same, the search process is consistent with the single-infeed HVDC system. Hence, a typical search process with different selected HVDC system is introduced. Take the fault ground impedance Z_f as the target parameter, whose range is $[\underline{Z}_f, \overline{Z}_f] = [0, 0.1]$p.u.. Set $\varepsilon_1 = 1\%$, $\varepsilon_2 = 1\%$. The fault is a three-phase impedance grounding fault at the Fengxian converter

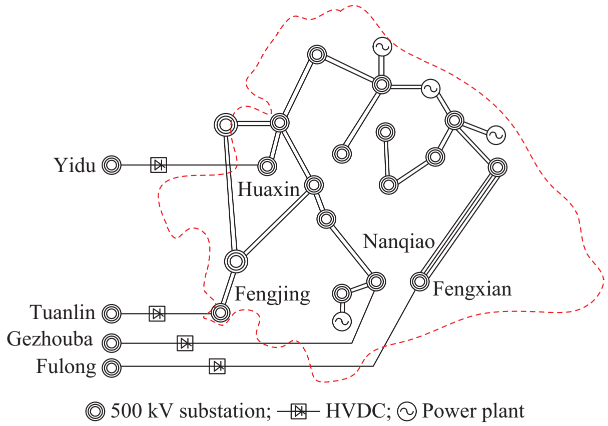

Fig. 14. 500 kV partial network structure of eastern china power grid.

bus with a duration of 0.1 s. Table V shows the search process of Z_f limit. Since the selected HVDC system from the first step to the third one in search process is the same, Fig. 15 only shows the extinction angle trajectories in the search process after the third iteration.

TABLE V
SEARCH PROCESS OF Z_f LIMIT

No.	Line	λ	$\underline{Z}_f$ (p.u.)	$\underline{\sigma}$ (%)	$\overline{Z}_f$ (p.u.)	$\overline{\sigma}$ (%)	$Z_{f.cr}^n$ (p.u.)	σ_{cr}^n (%)
1	GN	0.0021	0	−100.00	0.1000	97.19	0.0507	94.93
2	GN	0.0021	0	−100.00	0.0507	94.93	0.0260	89.05
3	GN	0.0021	0	−100.00	0.0260	89.05	0.0138	72.87
4	GN	0.0021	0	−100.00	0.0138	72.87	0.0080	26.62
5	FF	0.0020	0	−100.00	0.0080	26.62	0.0063	−26.11
6	GN	0.0016	0.0063	−26.11	0.0080	25.38	0.0071	0.91

Except for selecting HVDC system, the search process for multi-infeed HVDC system is similar to the single-infeed HVDC system. It can be observed that the selected HVDC system from the first to third iteration is the HVDC line of GN, but the selected HVDC system near the critical parameter is the HVDC line of FF. When $Z_{f.cr}^6 = 0.0071$ p.u., $\sigma_{cr}^4 = 0.91\%$ is less than ε_2, then the search is over. This search method ensures the monotonicity of the index-parameter is not affected by the complex factors of the multiple CFs during the entire search process, which guarantees the convergence.

Similar to the test cases of single-infeed HVDC system, 30 sets of examples are randomly selected for the above 3 typical parameters (10 sets respectively) in this multiple-infeed HVDC system to verify the effectiveness of the proposed strategy. Table VI shows that the computation cost of the proposed search strategy is less than the dichotomy method for all the cases in this multi-infeed HVDC system. The convergence speed has been increased by 60%-100% on average. It demonstrates that the search strategy is applicable to large-scale AC/DC hybrid power systems.

It can be obtained from the above cases that CSMI is applicable to different parameters and commutation processes. The sensitivity information of the index can be used to search the parameter limit. The accuracy of the integral trajectory could ensure the accuracy of the parameter limit.

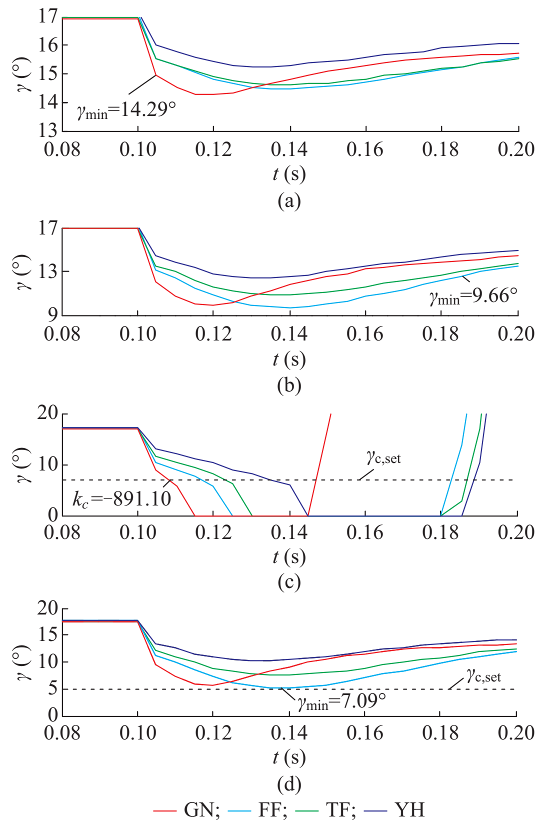

Fig. 15. Extinction angle trajectories in search for Z_f limit for multi-infeed HVDC system. (a) Extinction angle trajectories with $Z_{f.cr}^3 = 0.0138$ p.u.. (b) Extinction angle trajectories with $Z_{f.cr}^4 = 0.0080$ p.u.. (c) Extinction angle trajectories with $Z_{f.cr}^5 = 0.0063$ p.u.. (d) Extinction angle trajectories with $Z_{f.cr}^6 = 0.0071$ p.u..

TABLE VI
COMPARISON OF COMPUTATION COSTS IN MULTI-INFEED HVDC SYSTEM

Parameter	$\overline{N}_{SS}$	$\overline{N}_{BS}$	$\min(N_{SS})$	$\max(N_{SS})$	ζ
Z_f	7.4	12.0	6	9	1.62
P_d	5.7	10.6	4	8	1.98
τ	6.2	10.9	6	9	1.75

VI. CONCLUSION

This paper proposes a CSMI that can reflect the degree of commutation success/failure in a trustworthy manner based on the characteristic quantities of the extinction angle trajectory. This index not only meets the requirements of a quantifiable trajectory margin, but also considers the influence of arbitrary parameters and complex system configurations. Furthermore, we use the sensitivity information provided by the index to propose a search strategy for parameter limit. With guaranteed accuracy, this strategy greatly improves the convergence speed compared with the dichotomy method based on qualitative criteria. By varying the selection of faults and parameters, the rapidity and robustness of the proposed method is verified in a modified IEEE 39-bus system and a practical multi-infeed HVDC system.

The proposed index and the corresponding parameter limit search strategy can be used to reduce the update cycle of on-line security analysis programs and improve the adaptability of security controls to system operation conditions. The index is also conducive to the in-depth quantitative analysis of the adverse effect mechanism of the commutation process with parameter variations. The optimized operation of the AC/DC hybrid power system can be achieved by quantitative analysis, contributing to the security and economic coordination in cross-region energy transmission.

References

[1] J. M. Maza-Ortega, E. Acha, S. García *et al.*, "Overview of power electronics technology and applications in power generation transmission and distribution," *Journal of Modern Power Systems and Clean Energy*, vol. 5, no. 4, pp. 499-514, Jul. 2017.

[2] D. Huang, Y. Shu, J. Ruan *et al.*, "Ultra high voltage transmission in China: developments, current status and future prospects," *Proceedings of the IEEE*, vol. 97, no. 3, pp. 555-583, Mar. 2009.

[3] Y. Xue, X. Zhang, and C. Yang, "Commutation failure elimination of LCC HVDC systems using thyristor-based controllable capacitors," *IEEE Transactions on Power Delivery*, vol. 33, no. 3, pp. 1448-1458, Jun. 2018.

[4] Y. Xue, X. Zhang, and C. Yang, "Series capacitor compensated AC filterless flexible LCC HVDC with enhanced power transfer under unbalanced faults," *IEEE Transactions on Power Systems*, vol. 34, no. 4, pp. 3069-3080, Jul. 2019.

[5] C. Guo, Z. Yang, B. Jiang *et al.*, "An evolved capacitor-commutated converter embedded with antiparallel thyristors based dual-directional full-bridge module," *IEEE Transactions on Power Delivery*, vol. 33, no. 2, pp. 928-937, Apr. 2018.

[6] H. Rao, S. Xu, Y. Zhao *et al.*, "Research and application of multiple STATCOMs to improve the stability of AC/DC power systems in China southern grid," *IET Generation, Transmission & Distribution*, vol. 10, no. 13, pp. 3111-3118, Oct. 2016.

[7] P. Wang, Q. Mou, X. Liu *et al.*, "Start-up control of a synchronous condenser integrated HVDC system with power electronics based static frequency converter," *IEEE Access*, vol. 7, pp. 146914-146921, Oct. 2019.

[8] J. Bauman and M. Kazerani, "Commutation failure reduction in HVDC systems using adaptive fuzzy logic controller," *IEEE Transactions on Power Systems*, vol. 22, no. 4, pp. 1995-2002, Nov. 2007.

[9] H. Son and H. Kim, "An algorithm for effective mitigation of commutation failure in high-voltage direct-current systems," *IEEE Transactions on Power Delivery*, vol. 31, no. 4, pp. 1437-1446, Aug. 2016.

[10] Z. Wei, Y. Yuan, X. Lei *et al.*, "Direct-current predictive control strategy for inhibiting commutation failure in HVDC converter," *IEEE Transactions on Power Systems*, vol. 29, no. 5, pp. 2409-2417, Sept. 2014.

[11] C. Guo, Y. Liu, C. Zhao *et al.*, "Power component fault detection method and improved current order limiter control for commutation failure mitigation in HVDC," *IEEE Transactions on Power Delivery*, vol. 30, no. 3, pp. 1585-1593, Jun. 2015.

[12] S. Mirsaeidi, X. Dong, D. Tzelepis *et al.*, "A predictive control strategy for mitigation of commutation failure in LCC-based HVDC systems," *IEEE Transactions on Power Electronics*, vol. 34, no. 1, pp. 160-172, Jan. 2019.

[13] Y. Tang, C. Zheng, B. Lou *et al.*, "Research on DC power control strategy for mitigating continuous commutation failure," *Power System Technology*, vol. 43, no. 10, pp. 3514-3522, Oct. 2019.

[14] Y. Zhang, Y. Jiang, X. Qin *et al.*, "The research on the countermeasure via fast decrease of DC power reference to alleviate DC blockdown risk due to successive commutation failure," *Power System Technology*, vol. 43, no. 10, pp. 3569-3577, Oct. 2019.

[15] C. V. Thio, J. B. Davies, and K. L. Kent, "Commutation failures in HVDC transmission systems," *IEEE Transactions on Power Delivery*, vol. 11, no. 2, pp. 946-957, Apr. 1996.

[16] J. Xu, H. Tan, H. Sun *et al.*, "Research on method to analyze commutation failure in HVDC power transmission system considering the impact of DC current variation and occurrence moment of AC fault," *Power System Technology*, vol. 39, no. 5, pp.1261-1267, May 2015.

[17] F. Wang, T. Liu, X. Li *et al.*, "Commutation failure analysis considering DC current rising and voltage drop speed," *Automation Electric Power Systems*, vol. 40, no. 22, pp. 111-117, Nov. 2016.

[18] Y. Shao and Y. Tang, "Fast evaluation of commutation failure risk in multi-infeed HVDC systems," *IEEE Transactions on Power Systems*, vol. 33, no. 1, pp. 646-653, Jan. 2018.

[19] E. Rahimi, A. M. Gole, J. B. Davies *et al.*, "Commutation failure in single- and multi-infeed HVDC systems," in *Proceedings of 8th IEE International Conference on AC and DC Power Transmission*, London, UK, Jun. 2006, pp. 182-186.

[20] X. Chen, A. M. Gole, and C. Guo, "A fast calculation method for the local commutation failure immunity indices in single- and multi-infeed HVDC systems," in *Proceedings of 11th IET International Conference on AC and DC Power Transmission*, Birmingham, UK, Jul. 2015, pp. 1-6.

[21] H. Xiao, Y. Li, J. Zhu *et al.*, "Efficient approach to quantify commutation failure immunity levels in multi-infeed HVDC systems," *IET Generation, Transmission & Distribution*, vol. 10, no. 4, pp. 1032-1038, Mar. 2016.

[22] H. Yang, Z. Cai, X. Li *et al.*, "Assessment of commutation failure in HVDC systems considering spatial-temporal discreteness of AC system faults," *Journal of Modern Power Systems and Clean Energy*, vol. 6, no. 5, pp. 1055-1065, Sept. 2018.

[23] Y. Xue, *Quantitative Study of General Motion Stability and an Example on Power System Stability*. Nanjing, China: Jiangsu Technology Press, 1999, pp. 234-246.

[24] Y. Xue, T. Xu, B. Liu *et al.*, "Quantitative assessments for transient voltage security," *IEEE Transactions on Power Systems*, vol. 15, no. 3, pp. 1077-1083, Aug. 2000.

[25] T. Xu and Y. Xue, "Quantitative assessments of transient frequency deviation acceptability," *Automation Electric Power Systems*, vol. 26, no. 19, pp. 7-10, Oct. 2002.

[26] Y. Xue, Y. Luo, F. Xue *et al.*, "On-line transient stability assessment in operation-DEEAC in northeast China power system," in *Proceedings of TENCON'93. IEEE Region 10 International Conference on Computers, Communications and Automation*, Beijing, China, Oct. 1993, pp. 72-76.

[27] Y. Xue, "Space-time cooperative framework for defending blackouts: Part two reliable information, quantitative analysis and adaptive controls," *Automation Electric Power Systems*, vol. 30, no. 2, pp. 1-10, Jan. 2006.

[28] A. Blicher, *Thyristor Physics*. New York: Springer-Verlag, 1964, pp. 88-97.

[29] *Terminology for High-voltage Direct Current (HVDC) Transmission*, IEC 60633, 2015.

[30] J. Arrillaga, *High Voltage Direct Current Transmission*, 2nd ed., London: Institution of Engineering and Technology, 2008, pp. 201-206.

[31] J. Karlsson, "Simplified control model for HVDC classic," M.S. thesis, Department of Electrical Systems, Royal Institute of Technology, Stockholm, Sweden, 2006.

[32] D. Lu, Y. Wang, Z. Wang *et al.*, "Inverter maximum alpha control in UHVDC transmission with hierarchical connection mode," *Proceedings of the CSEE*, vol. 36, no. 7, pp. 1808-1816, Apr. 2016.

[33] J. Liu, X. Li, C. Wu *et al.*, "Research on critical index of commutation failure in HVDC system," *Power System Technology*, vol. 33, no. 08, pp. 8-12, Apr. 2009.

[34] E. Rahimi, S. Filizadeh, and A. M. Gole, "Commutation failure analysis in HVDC systems using advanced multiple-run methods," in *Proceedings of 6th International Conference on Power Systems Transients*, Montreal, Canada, Jun. 2005, pp. 1-5.

[35] Y. Wang, X. Han, D. Sun *et al.*, "Analysis on voltage stability of receiving grid considering control strategy of DC transmission line," *Automation of Electric Power Systems*, vol. 40, no. 6, pp. 35-41, Mar. 2016.

Qi Tao received her B.E. degree from Southeast University, Nanjing, China, in 2013. Currently, she is pursuing her Ph.D. degree in Zhejiang University, Hangzhou, China. Her research interests include HVDC transmission, power system analysis and control.

Yusheng Xue received the B.E. degree from Shandong University, Jinan, China, in 1963, and the M.S. degree from State Grid Electric Power Research Institute, Nanjing, China, in 1981, respectively. He received the Ph.D. degree in electrical engineering from University of Liège, Liège, Belgium, in 1987. He is a member of Chinese Academy of Engineering, Honorary President of State Grid Electric Power Research Institute (NARI Group Corporation), and professor in the Electrical Engineering Department, Shandong University. His research interest includes power system automation.